Solid State Communications 169 (2013) 24–27

Contents lists available at SciVerse ScienceDirect

Solid State Communications

journal homepage: www.elsevier.com/locate/ssc

Fast-track Communication

Displacive lattice excitation through nonlinear phononics viewed by femtosecond X-ray diffraction

M. Först [a,*], R. Mankowsky [a], H. Bromberger [a], D.M. Fritz [b], H. Lemke [b], D. Zhu [b], M. Chollet [b], Y. Tomioka [c], Y. Tokura [d], R. Merlin [e], J.P. Hill [f], S.L. Johnson [g], A. Cavalleri [a,h,**]

[a] Max-Planck Institute for the Structure and Dynamics of Matter, 22761 Hamburg, Germany
[b] Linac Coherent Light Source, SLAC National Accelerator Laboratory, Menlo Park, CA 94025, USA
[c] Correlated Electron Engineering Group, AIST, Tsukuba, Ibaraki 305-8562, Japan
[d] Department of Applied Physics, University of Tokyo, Tokyo 113-8656, Japan
[e] Department of Physics, University of Michigan, Ann Arbor, MI 48109, USA
[f] Condensed Matter Physics and Materials Science Department, Brookhaven National Laboratory, Upton, NY 11973, USA
[g] Institute for Quantum Electronics, Physics Department, ETH Zürich, 8093 Zürich, Switzerland
[h] Department of Physics, University of Oxford, Oxford OX1 3PU, United Kingdom

ARTICLE INFO

Article history:
Received 14 June 2013
Received in revised form
24 June 2013
Accepted 26 June 2013
by A. Pinczuk
Available online 4 July 2013

Keywords:
A. Correlated electron systems
D. Ionic Raman Scattering
D. Nonlinear phononics
E. Time-resolved hard X-ray diffraction

ABSTRACT

The nonlinear lattice dynamics of $La_{0.7}Sr_{0.3}MnO_3$, as initiated by strong mid-infrared femtosecond pulses made resonant with a specific lattice vibration, are measured with ultrafast X-ray diffraction at the LCLS free electron laser. Our experiments show that large amplitude excitation of an infrared-active stretching mode leads also to a displacive motion along the coordinate of a second, anharmonically coupled, Raman mode. This rectification of the vibrational field is described within the framework of the Ionic Raman Scattering theory and explains how direct lattice excitation in the nonlinear regime can induce a structural phase transition.

1. Introduction

Selective excitation of infrared-active lattice vibrations has led to new avenues for the control of quantum matter. Insulator–metal transitions [1–4] and even high-temperature superconductivity [5] have been induced in this way. Such vibrational stimulation differs significantly from carrier excitation in the near-infrared [6,7], and makes possible the control of solids in their electronic ground state. The reduced dissipation of direct lattice excitation makes it also attractive for applications in functional material control.

Despite all these striking observations, until recently it has been difficult to understand how an infrared field, which drives atomic motions with zero average displacement about the equilibrium crystal structure, could induce a long lived change in the properties of the system other than heating. A working hypothesis was derived from recent all-optical experiments [8], which indicated that the underlying structural dynamics can be described by the theory of Ionic Raman Scattering (IRS) [9–11]. In the IRS process, the oscillatory motion of a resonantly excited infrared-active mode couples nonlinearly to a Raman-active distortion. As lattice anharmonicities that scale with the square of the phonon coordinate Q_{IR} can cause rectification of the vibrational field (similar to optical rectification in nonlinear optics), a displacive force can be exerted onto the crystal lattice in this way [8]. In the specific case of $La_{0.7}Sr_{0.3}MnO_3$, the structural pathway is believed to involve a conversion from optically driven Mn–O stretching vibrations into rotations of oxygen octahedra. This motion is especially important in the manganites as it can control the Mn–O–Mn bond angle, which strongly influences the electronic and magnetic properties [12].

From the optical probe experiments in $La_{0.7}Sr_{0.3}MnO_3$, the frequency and the symmetry of a coherently excited Raman mode excitation could be extracted. But the one key phenomenon of a displacive force that drives the crystal structure into a new transient conformation could not be proven. Indeed, from the analysis of the optical data alone, it is not possible to uniquely establish if the Raman-mode oscillations occur around the atomic positions of the unperturbed ground state or around those of a displaced crystal structure.

To demonstrate the existence of a displacement, we make use of femtosecond X-ray pulses to measure the ultrafast evolution of those weak Bragg reflections that are exclusively sensitive to the

* Corresponding author. Tel.: +49 40 8998 5360.
** Corresponding author at: Max-Planck Institute for the Structure and Dynamics of Matter, 22761 Hamburg, Germany.
E-mail addresses: michael.foerst@mpsd.cfel.de (M. Först), andrea.cavalleri@mpsd.cfel.de (A. Cavalleri).

0038-1098/$ - see front matter © 2013 Elsevier Ltd. All rights reserved.
http://dx.doi.org/10.1016/j.ssc.2013.06.024

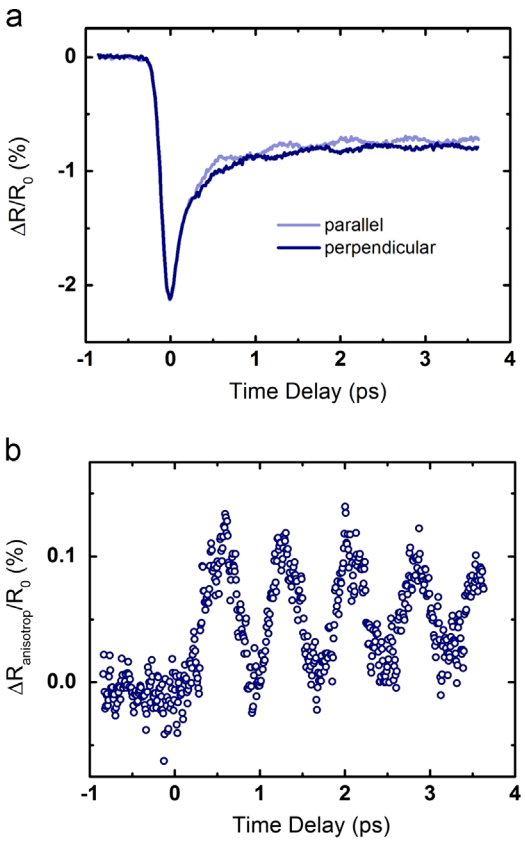

Fig. 1. (Color online) Time-resolved optical spectroscopy: (a) time-resolved reflectivity changes following resonant excitation of the E_u symmetry Mn–O stretching vibration in $La_{0.7}Sr_{0.3}MnO_3$. Mid-infrared 120-fs light pulses at 14.3 μm (2.5 μm FWHM) were focused onto the sample providing an excitation fluence of 2 mJ/cm^2. The probe polarization at 800 nm wavelength has been set parallel (light blue) and perpendicular (dark blue) to the pump polarization. The E_g phonon induced oscillatory signal contributions at 1.2 THz frequency are 180° out-of-phase for the different polarizations and (b) Raman phonon-induced anisotropic contributions to the transient reflectivity obtained by subtracting the two signals shown in part (a).

oxygen positions [13–18]. Note that this feat is uniquely made possible by the high X-ray flux of the free electron laser and would not be observable using weaker femtosecond X-ray sources. By measuring a long-lived change in two structure factors, we prove that the mechanism of nonlinear lattice control involves a displacement of the atoms, with a quantitative agreement to the predictions of the Ionic Raman Scattering theory.

Fig. 1 summarizes the information that can be retrieved from optical probe experiments (see also Ref. [8] for details). Oscillations at 1.2 THz follow resonant excitation of the 18-THz Mn–O stretching vibration with E_u symmetry [19,20]. The polarization dependence confirms that the observed Raman-active mode has E_g symmetry [21,22]. Note that an offset in the lattice coordinates is qualitatively consistent with the data of Fig. 1(b), where a long-lived step results after the polarization independent response has been subtracted from the transient reflectivity. However, heating or other long-lived effect may also explain this step.

Atomic motions along optical phonon coordinates result in a change of the X-ray scattering structure factor, thus modulating the intensity of Bragg peaks [14]. As shown in Fig. 2(b), the E_g Raman mode corresponds to rotations of adjacent MnO_6 octahedra around an axis (red arrow) orthogonal to the rhombohedral [111] direction (blue arrow) [19,22,23]. In $La_{0.7}Sr_{0.3}MnO_3$, the {201} family of reflections is forbidden in the Mn and La/Sr sublattices, and is therefore solely sensitive to the motions of the oxygen atoms. We note that these reflections are also very weak and the only femtosecond X-ray source with sufficient flux to observe them is a free electron laser.

The femtosecond X-ray diffraction experiments discussed here were performed at the XPP beamline of the Linac Coherent Light Source (LCLS) free electron laser [24]. The crystal was excited by 220-fs mid-infrared pulses at 15 μm wavelength. The incident excitation fluence was 1.2 mJ/cm^2. X-ray probe pulses, estimated to be < 70 fs in duration, were generated by the free electron laser. The experiment was carried out at a repetition rate of 120 Hz. A silicon (111) monochromator was used to select the 6 keV probe pulse energy. Non-coplanar time dependent diffraction from the (201) and (012) lattice reflections was measured at an incidence

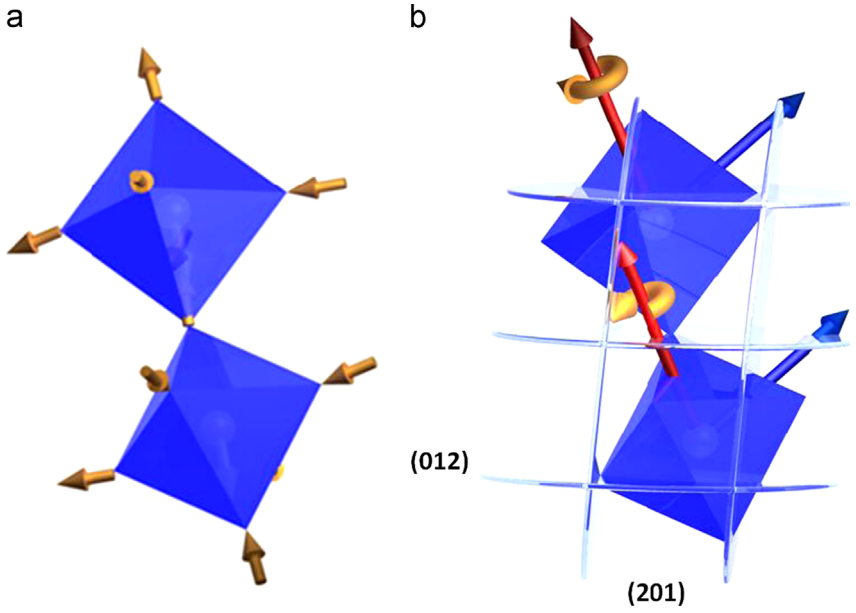

Fig. 2. (Color online) Phonon modes and Bragg planes: illustration of two adjacent oxygen octahedra in $La_{0.7}Sr_{0.3}MnO_3$, a rhombohedrally distorted perovskite of point group D^6_{3d}. (a) Atomic motion associated with the infrared-active Mn–O stretching vibration of E_u symmetry, according to Ref. [20] and (b) Sketch of the nonlinearly driven Raman-active E_g mode, a rotation of these oxygen octahedra around an axis (red arrow) perpendicular to the rhombohedral [111] direction (blue arrow). These atomic motions lead to an increase and decrease in scattering efficiencies at the (012) and (201) Bragg planes, respectively.

angle of 5°, chosen to match the X-ray penetration depth to that of the mid-infrared pump pulses. Shot-to-shot normalization to the X-ray pulse energy after the monochromator corrected the detected signals for intensity and wavelength fluctuations from the free electron laser. The time resolution of the experiment was 300 fs, as limited by the timing jitter between the mid-infrared and X-ray pulses.

Fig. 3 shows the time-delay dependent relative changes in scattered intensity from the (012) and (201) lattice reflections after resonant excitation of the Mn–O stretching vibration. Two step-like responses of opposite sign are observed. By fitting the data with error functions, relative scattering changes $\Delta I/I_0$ of +0.28% ($\pm$0.02%) and −0.66% ($\pm$0.05%) are derived, respectively.

To deduce the atomic displacement along the E_g phonon coordinate from the changes in scattered intensity, we compare the measured signals to the formula for the specific structure factors [25]. Specifically, $F_{hkl}=\sum_j f_j \exp(-i\boldsymbol{G}_{hkl}\cdot\boldsymbol{r}_j)$ with $\boldsymbol{G}_{hkl}$ the reciprocal lattice vectors associated with the (hkl) diffraction peaks, f_j the atomic scattering factors and $\boldsymbol{r}_j$ the positions of the j-th atom in the unit cell. The transient atom positions are obtained by displacements from the equilibrium positions $\boldsymbol{r}_j^{(0)}$ with amplitude Q_{RS} along the eigenvector $\boldsymbol{e}_j$ of the E_g mode, i.e. $\boldsymbol{r}_j=\boldsymbol{r}_j^{(0)}+Q_{RS}\boldsymbol{e}_j$.

For lattice distortions considerably smaller than interatomic distances, the change ΔI in scattered intensity $I\sim|F|^2$ is to leading order linearly proportional to the normal coordinate Q_{RS}. Atomic motion along the E_g coordinate, as nonlinearly excited in our experiment and shown in Fig. 2(a), results in calculated relative intensity changes $(\Delta I/I_0)/Q_{RS}$ of +0.043 pm^{-1} and −0.057 pm^{-1} for the (012) and (201) Bragg peaks, respectively. We divide the measured $\Delta I/I_0$ by the coefficients above and average over the results of the two peaks. In this way, we extract displacement along the phonon eigenvector of about Q_{RS}=0.09 pm, which is equivalent to rotations of the oxygen octahedra of 0.035°.

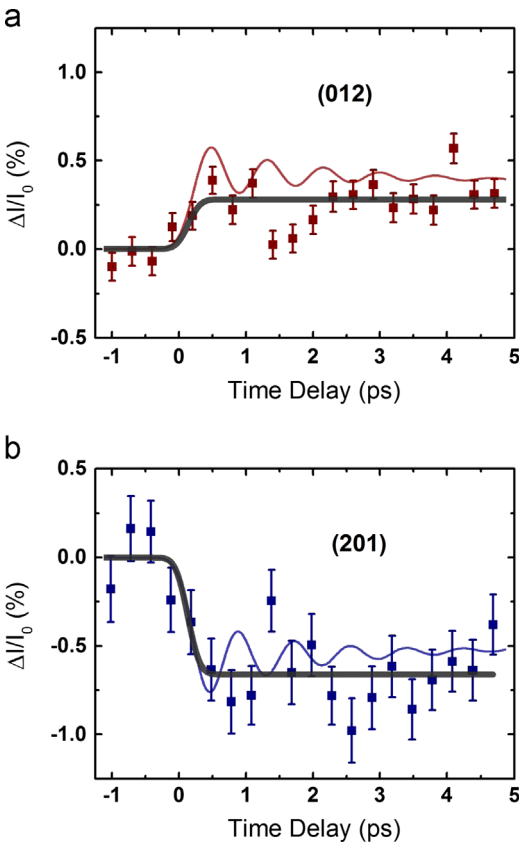

Fig. 3. (Color online) Time-resolved X-ray diffraction: time-resolved changes in scattered intensity from the (012) and (201) lattice reflections in $La_{0.7}Sr_{0.3}MnO_3$, following resonant excitation of the Mn–O stretching vibration in the mid-infrared. The error bars are calculated from photon statistics. The Bragg peaks are sensitive to the E_g symmetry rotational Raman mode. The gray solid lines are error functions fitted to the data. The color lines are results of Q_{RS}, calculated from the coupled differential Equations (1) and (2) and multiplied by the coefficients $(\Delta I/I_0)/Q_{RS}$ for the respective lattice reflections. Here, the anharmonic constant A is the only parameter that has been adapted to fit the calculations to the experimental data.

According to the IRS theory, the nonlinear interaction between the resonantly driven infrared-active vibration and the Raman-active mode is described by the Hamilton operator $H_A=-NAQ_{IR}^2Q_{RS}$. Here, Q_{IR} is the normal coordinate of the IR-mode, A is the anharmonic coupling constant between the two modes and N is the number of unit cells [10]. The classical equations of motion of the coupled oscillators with frequencies Ω_{IR} and Ω_{RS} are

$$\mu_{IR}(\ddot{Q}_{IR}+2\gamma_{IR}\dot{Q}_{IR}+\Omega_{IR}^2Q_{IR})=AQ_{IR}Q_{RS}+f(t) \quad (1)$$

and

$$\mu_{RS}(\ddot{Q}_{RS}+2\gamma_{RS}\dot{Q}_{RS}+\Omega_{RS}^2Q_{RS})=AQ_{IR}^2 \quad (2)$$

where μ_i are the effective masses, and γ_i the damping rates. The driving force on the IR mode is given by the incident laser pulse through $f(t)=e^*E_0\sin(\omega_L t)\exp(-2\ln(2)t^2/{\tau_L}^2)$, with e^* the effective charge, E_0 the peak electric field, ω_L the laser frequency, and τ_L the pulse duration (FWHM).

In centrosymmetric crystals the Raman modes are even, thus they cannot be excited directly by light. Instead, they are non-linearly driven by a term proportional to the amplitude squared of the IR-active vibration. The excitation is prompt, if the Raman frequency Ω_{RS} is considerably smaller than, both, the IR-mode frequency Ω_{IR} and the inverse laser pulse duration $1/\tau_L$. In this case, the normal coordinate Q_{RS} is predicted to oscillate coherently around a new equilibrium position [8], as observed qualitatively in Fig. 1(b).

The color lines plotted in Fig. 3 represent the results of the numerical solution of the coupled differential Equations (1) and (2). For these plots, the calculated transient E_g mode amplitude Q_{RS} was multiplied by the coefficients $(\Delta I/I_0)/Q_{RS}$ for the respective lattice reflections and convolved with a Gaussian of 300 fs FWHM to take into account the timing jitter between the pump and probe pulses. The anharmonic constant A is the only parameter that has been chosen to best fit these calculations to the experimental data. We find $A=6.4\times10^{12}$ g/(cm s^2) and an E_g phonon displacement of 0.1 pm which corresponds to relative intensity changes of about +0.4% and −0.55% in the (012) and (201) diffraction peaks. These calculated transient diffraction changes deviate only slightly from the error function fits and the experimental data. The coherent oscillations could be observed in the measurements if the signal to noise ratio was reduced far below 0.1%, which is not realistic for these weak reflections.

Alternative scenarios fail to describe our experimental data. The amplitude Q_{IR} of the resonantly driven infrared-active E_u mode oscillates around its equilibrium position with no net displacement. With the given time resolution of this experiment no intensity change is expected for the (012) and (201) diffraction peaks. Secondly, heating of the crystal lattice may happen already on the sub-picosecond time scale, although this effect reduces the diffraction intensity for all peaks, according to the Debye–Waller factor. Thus, the observed increase at the (012) diffraction peak clearly excludes heating as an explanation.

Finally, we compare the measured value for the anharmonic constant A to an order-of-magnitude estimate for the IRS mediated coupling between distinct phonon modes in quartz. Martin and Genzel argued that equal harmonic and anharmonic contributions to the lattice potential energy $U=N\sum\frac{1}{2}\mu_i\Omega_i^2Q_i^2+NAQ_{IR}^2Q_{RS}$ are to be expected for atomic displacements of order the interatomic distances [10]. Adapting this argument to the nonlinear coupling

of the infrared-active E_u to the Raman-active E_g mode in $La_{0.7}Sr_{0.3}MnO_3$, one estimates $A=6\times10^{12}$ g/(cm s^2), which is reassuringly comparable to the experimentally determined value $A^{(exp)}=6.4\times10^{12}$ g/(cm s^2).

In summary, the present femtosecond X-ray diffraction study demonstrates the displacive reaction of a crystal lattice driven to large amplitudes by mid-infrared radiation. The relative change of the two peaks analyzed, quantitatively substantiates the applicability of Ionic Raman Scattering theory to mid-infrared control of the solid state. We note that in the related single-layered compound $La_{0.5}Sr_{1.5}MnO_4$, we recently suggested that vibrationally induced melting of the charge/orbital and magnetic order parameters could be explained by a quench of exchange interactions caused by IRS excitation of the Jahn–Teller distortion [3]. The present work explicitly supports this earlier assignment. More generally, the ability to quantify nonlinear lattice dynamics with femtosecond X-rays paves the way towards predictively accurate design of lattice control experiments. Pressure-like effects along selected normal mode coordinates could be achieved in this way, with the ability to control the electronic properties of quantum matter [12,26]on the ultrafast time scale.

Acknowledgment

Work performed at Brookhaven National Laboratory was supported by the US Department of Energy, Division of Materials Science, under Contract no. DE-AC02-98CH10886.

Portions of this research were carried out at the Linac Coherent Light Source (LCLS) at the SLAC National Accelerator Laboratory. LCLS is an Office of Science User Facility operated for the U.S. Department of Energy Office of Science by Stanford University.

References

[1] M. Rini, R. Tobey, N. Dean, J. Itatani, Y. Tomioka, Y. Tokura, R.W. Schoenlein, A. Cavalleri, Nature 449 (2007) 72.
[2] R. Tobey, D. Prabhakaran, A.T. Boothroyd, A. Cavalleri, Phys. Rev. Lett. 101 (2008) 197404.
[3] M. Först, R.I. Tobey, S. Wall, H. Bromberger, V. Khanna, A.L. Cavalieri, Y.-D. Chuang, W.S. Lee, R. Moore, W.F. Schlotter, J.J. Turner, O. Krupin, M. Trigo, M. Zheng, J.F. Mitchell, S.S. Dhesi, J.P. Hill, A. Cavalleri, Phys. Rev. B 84 (2011) 241104.
[4] A.D. Caviglia, R. Scherwitzl, P. Popovich, W. Hu, H. Bromberger, R. Singla, M. Mitrano, M.C. Hoffmann, S. Kaiser, P. Zubko, S. Gariglio, J.M. Triscone, M. Först, A. Cavalleri, Phys. Rev. Lett. 108 (2012) 136801.
[5] D. Fausti, R.I. Tobey, N. Dean, S. Kaiser, A. Dienst, M.C. Hoffmann, S. Pyon, T. Takayama, H. Takagi, A. Cavalleri, Science 331 (2011) 189.
[6] K. Miyano, K. Tanaka, Y. Tomioka, Y. Tokura, Phys. Rev. Lett. 78 (1997) 4257.
[7] M. Fiebig, K. Miyano, Y. Tomioka, Y. Tokura, Science 280 (1925) (1998).
[8] M. Först, C. Manzoni, S. Kaiser, Y. Tomioka, Y. Tokura, R. Merlin, A. Cavalleri, Nat. Phys. 7 (2011) 854.
[9] R.F. Wallis, A.A. Maradudin, Phys. Rev. B 3 (1971) 2063.
[10] T.P. Martin, L. Genzel, Phys. Stat. Sol. B 61 (1974) 493.
[11] D.L. Mills, Phys. Rev. B 35 (1987) 9278.
[12] H.Y. Hwang, S.-W. Cheong, P.G. Radaelli, M. Marezio, B. Battlog, Phys. Rev. Lett. 75 (1995) 914.
[13] A.M. Lindenberg, et al., Science 308 (2005) 392.
[14] K. Sokolowski-Tinten, C. Blome, J. Blums, A. Cavalleri, C. Dietrich, A. Tarasevitch, I. Uschmann, E. Förster, M. Kammler, M.H. von Hoengen, D. von der Linde, Nature 422 (2003) 287.
[15] D.M. Fritz, et al., Science 315 (2007) 633.
[16] P. Beaud, S.L. Johnson, E. Vorobeva, U. Staub, R.A. De Souza, C.J. Milne, Q.X. Jia, G. Ingold, Phys. Rev. Lett. 103 (2009) 155702.
[17] S.L. Johnson, P. Beaud, E. Vorobeva, C.J. Milne, E.D. Murray, S. Fahy, G. Ingold, Phys. Rev. Lett. 102 (2009) 175503.
[18] S.L. Johnson, E. Vorobeva, P. Beaud, C.J. Milne, G. Ingold, Phys. Rev. Lett. 103 (2009) 205501.
[19] Y. Okimoto, T. Katsufutji, T. Ishikawa, T. Arima, Y. Tokura, Phys. Rev. B 55 (1997) 4206.
[20] M.V. Abrashev, A.P. Litvinchuk, M.N. Iliev, R.L. Meng, V.N. Popov, V.G. Ivanov, R.A. Chakalov, C. Thomsen, Phys. Rev. B 59 (1999) 4146.
[21] E. Granado, N.O. Moreno, A. Garcia, J.A. Sanjurjo, C. Rettori, I. Torriani, S.B. Oseroff, J.J. Neumeier, K.J. McClellan, S.-W. Cheong, Y. Tokura, Phys. Rev. B 58 (1998) 11435.
[22] M.N. Iliev, M.V. Abrashev, J. Raman Spectrosc. 32 (2001) 805.
[23] In general, the E_g modes are a two-dimensional space of degenerate modes. The direction of the particular rotation axis (red arrow) drawn here corresponds to the E_g mode nonlinearly excited in the diffraction experiment described below.
[24] P. Emma, et al., Nat. Photonics 4 (2010) 641.
[25] B.E. Warren, X-ray Diffraction, Dover Publications, New York, 2009.
[26] M. Ido, N. Yamada, M. Oda, Y. Segawa, N. Momono, A. Onodera, Y. Okajima, K. Yamada, Physica C 185–189 (1991) 911.